

# First Detection of sub-PeV Diffuse Gamma Rays from the Galactic Disk: Evidence for Ubiquitous Galactic Cosmic Rays beyond PeV Energies

M. Amenomori,<sup>1</sup> Y. W. Bao,<sup>2</sup> X. J. Bi,<sup>3</sup> D. Chen<sup>§,4</sup> T. L. Chen,<sup>5</sup> W. Y. Chen,<sup>3</sup> Xu Chen,<sup>3</sup> Y. Chen,<sup>2</sup> Cirennima,<sup>5</sup> S. W. Cui,<sup>6</sup> Danzengluobu,<sup>5</sup> L. K. Ding,<sup>3</sup> J. H. Fang,<sup>3,7</sup> K. Fang,<sup>3</sup> C. F. Feng,<sup>8</sup> Zhaoyang Feng,<sup>3</sup> Z. Y. Feng,<sup>9</sup> Qi Gao,<sup>5</sup> Q. B. Gou,<sup>3</sup> Y. Q. Guo,<sup>3</sup> Y. Y. Guo,<sup>3</sup> H. H. He,<sup>3</sup> Z. T. He,<sup>6</sup> K. Hibino,<sup>10</sup> N. Hotta,<sup>11</sup> Haibing Hu,<sup>5</sup> H. B. Hu,<sup>3</sup> J. Huang<sup>†,3</sup> H. Y. Jia,<sup>9</sup> L. Jiang,<sup>3</sup> H. B. Jin,<sup>4</sup> K. Kasahara,<sup>12</sup> Y. Katayose,<sup>13</sup> C. Kato,<sup>14</sup> S. Kato,<sup>15</sup> K. Kawata\*,<sup>15</sup> W. Kihara,<sup>14</sup> Y. Ko,<sup>14</sup> M. Kozai,<sup>16</sup> Labaciren,<sup>5</sup> G. M. Le,<sup>17</sup> A. F. Li,<sup>18,8,3</sup> H. J. Li,<sup>5</sup> W. J. Li,<sup>3,9</sup> Y. H. Lin,<sup>3,7</sup> B. Liu,<sup>19</sup> C. Liu,<sup>3</sup> J. S. Liu,<sup>3</sup> M. Y. Liu,<sup>5</sup> W. Liu,<sup>3</sup> Y.-Q. Lou,<sup>20,21,22</sup> H. Lu,<sup>3</sup> X. R. Meng,<sup>5</sup> K. Munakata,<sup>14</sup> H. Nakada,<sup>13</sup> Y. Nakamura,<sup>3</sup> H. Nanjo,<sup>1</sup> M. Nishizawa,<sup>23</sup> M. Ohnishi,<sup>15</sup> T. Ohura,<sup>13</sup> S. Ozawa,<sup>24</sup> X. L. Qian,<sup>25</sup> X. B. Qu,<sup>26</sup> T. Saito,<sup>27</sup> M. Sakata,<sup>28</sup> T. K. Sako,<sup>15</sup> J. Shao,<sup>3,8</sup> M. Shibata,<sup>13</sup> A. Shiomi,<sup>29</sup> H. Sugimoto,<sup>30</sup> W. Takano,<sup>10</sup> M. Takita<sup>¶,15</sup> Y. H. Tan,<sup>3</sup> N. Tateyama,<sup>10</sup> S. Torii,<sup>31</sup> H. Tsuchiya,<sup>32</sup> S. Udo,<sup>10</sup> H. Wang,<sup>3</sup> H. R. Wu,<sup>3</sup> L. Xue,<sup>8</sup> Y. Yamamoto<sup>†,28</sup> Z. Yang,<sup>3</sup> Y. Yokoe,<sup>15</sup> A. F. Yuan,<sup>5</sup> L. M. Zhai,<sup>4</sup> H. M. Zhang,<sup>3</sup> J. L. Zhang,<sup>3</sup> X. Zhang,<sup>2</sup> X. Y. Zhang,<sup>8</sup> Y. Zhang,<sup>3</sup> Yi Zhang,<sup>33</sup> Ying Zhang,<sup>3</sup> S. P. Zhao,<sup>3</sup> Zhaxisangzhu,<sup>5</sup> and X. X. Zhou<sup>9</sup>

(The Tibet AS $\gamma$  Collaboration)

<sup>1</sup>Department of Physics, Hirosaki University, Hirosaki 036-8561, Japan

<sup>2</sup>School of Astronomy and Space Science, Nanjing University, Nanjing 210093, China

<sup>3</sup>Key Laboratory of Particle Astrophysics, Institute of High Energy Physics, Chinese Academy of Sciences, Beijing 100049, China

<sup>4</sup>National Astronomical Observatories, Chinese Academy of Sciences, Beijing 100012, China

<sup>5</sup>Physics Department of Science School, Tibet University, Lhasa 850000, China

<sup>6</sup>Department of Physics, Hebei Normal University, Shijiazhuang 050016, China

<sup>7</sup>University of Chinese Academy of Sciences, Beijing 100049, China

<sup>8</sup>Institute of Frontier and Interdisciplinary Science and Key Laboratory of Particle Physics and Particle Irradiation (MOE), Shandong University, Qingdao 266237, China

<sup>9</sup>Institute of Modern Physics, SouthWest Jiaotong University, Chengdu 610031, China

<sup>10</sup>Faculty of Engineering, Kanagawa University, Yokohama 221-8686, Japan

<sup>11</sup>Faculty of Education, Utsunomiya University, Utsunomiya 321-8505, Japan

<sup>12</sup>Faculty of Systems Engineering, Shibaura Institute of Technology, Omiya 330-8570, Japan

<sup>13</sup>Faculty of Engineering, Yokohama National University, Yokohama 240-8501, Japan

<sup>14</sup>Department of Physics, Shinshu University, Matsumoto 390-8621, Japan

<sup>15</sup>Institute for Cosmic Ray Research, University of Tokyo, Kashiwa 277-8582, Japan

<sup>16</sup>Institute of Space and Astronautical Science, Japan Aerospace Exploration Agency (ISAS/JAXA), Sagami-hara 252-5210, Japan

<sup>17</sup>National Center for Space Weather, China Meteorological Administration, Beijing 100081, China

<sup>18</sup>School of Information Science and Engineering, Shandong Agriculture University, Taian 271018, China

<sup>19</sup>Department of Astronomy, School of Physical Sciences, University of Science and Technology of China, Hefei, Anhui 230026, China

<sup>20</sup>Department of Physics and Tsinghua Centre for Astrophysics (THCA), Tsinghua University, Beijing 100084, China

<sup>21</sup>Tsinghua University-National Astronomical Observatories of China (NAOC) Joint Research Center for Astrophysics, Tsinghua University, Beijing 100084, China

<sup>22</sup>Department of Astronomy, Tsinghua University, Beijing 100084, China

<sup>23</sup>National Institute of Informatics, Tokyo 101-8430, Japan

<sup>24</sup>National Institute of Information and Communications Technology, Tokyo 184-8795, Japan

<sup>25</sup>Department of Mechanical and Electrical Engineering, Shandong Management University, Jinan 250357, China

<sup>26</sup>College of Science, China University of Petroleum, Qingdao, 266555, China

<sup>27</sup>Tokyo Metropolitan College of Industrial Technology, Tokyo 116-8523, Japan

<sup>28</sup>Department of Physics, Konan University, Kobe 658-8501, Japan

<sup>29</sup>College of Industrial Technology, Nihon University, Narashino 275-8575, Japan

<sup>30</sup>Shonan Institute of Technology, Fujisawa 251-8511, Japan

<sup>31</sup>Research Institute for Science and Engineering, Waseda University, Tokyo 169-8555, Japan

<sup>32</sup>Japan Atomic Energy Agency, Tokai-mura 319-1195, Japan

<sup>33</sup>Key Laboratory of Dark Matter and Space Astronomy, Purple Mountain Observatory, Chinese Academy of Sciences, Nanjing 210034, China

(Dated: January 7, 2022)

We report, for the first time, the long-awaited detection of diffuse gamma rays with energies between 100 TeV and 1 PeV in the Galactic disk. Particularly, all gamma rays above 398 TeV are

observed apart from known TeV gamma-ray sources and compatible with expectations from the hadronic emission scenario in which gamma rays originate from the decay of  $\pi^0$ 's produced through the interaction of protons with the interstellar medium in the Galaxy. This is strong evidence that cosmic rays are accelerated beyond PeV energies in our Galaxy and spread over the Galactic disk.

## I. INTRODUCTION

Cosmic-ray energy spectrum has approximately a power-law shape  $dN/dE \propto E^p$  in an energy region between  $10^{10}$  eV and  $10^{20}$  eV [1]. One of the most prominent features of the spectrum is the so-called knee at  $4 \times 10^{15}$  eV ( $= 4$  PeV), where the spectrum steepens with its power-law index changing from  $p = -2.7$  to  $-3.1$  [2, 3]. In a scenario most widely accepted, cosmic rays are accelerated up to PeV energies by energetic objects in our Galaxy, such as supernova remnants (SNRs), and well confined in the Galaxy up to the knee energy by the Galactic magnetic field [4, 5], although source objects and acceleration mechanisms are still under discussion. To confirm the theory predicting the Galactic origin of the PeV cosmic rays, therefore, it would be conclusive to experimentally identify the objects in our Galaxy, called ‘‘PeVatrons’’, which are accelerating cosmic rays up to PeV energies.

In recent decades, high-energy gamma-ray observations have been utilized to identify cosmic-ray sources by detecting the arrival direction of gamma rays produced by cosmic rays, because gamma rays travel straight from the source free from the magnetic deflection. Through the hadronic interaction with ambient matters, PeV cosmic rays produce neutral pions which decay into gamma rays with energies as high as 100 TeV [6–8]. Recently, the ground-based Cherenkov telescopes and air shower (AS) arrays observed gamma rays with energies up to a few tens of TeV from more than 100 sources in the Galaxy [9–11]. The Tibet AS $\gamma$  [12] and HAWC experiments [13] also detected gamma rays beyond 100 TeV from a few sources which are very good candidates of PeVatrons. However, there has been no conclusive evidence for the cosmic-ray PeVatron reported so far.

Gamma-ray telescopes on board satellites, such as the EGRET and *Fermi*-LAT, have precisely observed diffuse gamma rays from the Galactic disk in an energy range  $0.1 < E < 100$  GeV [14, 15]. The gamma-ray distribution is extended more than a few degrees in Galactic latitude, similar to the distribution of interstellar gas. The measured spectra are now established to be dominated by emissions from the interaction of cosmic rays including electrons with interstellar gas and magnetic field in this energy region [15]. In the higher energy range, the Milagro experiment reported TeV diffuse gamma-ray emissions from the Cygnus region in the Galactic disk [16], while the ARGO-YBJ experiment reported diffuse gamma rays with  $0.35 < E < 2$  TeV extended over Galactic longitude ( $l$ ) between  $25^\circ < l < 100^\circ$  [17]. Overall, their observed fluxes are consistent with the standard *Fermi*-LAT model for the diffuse Galactic emission. At the highest energy region, the CASA-MIA experiment

presented the upper limits of Galactic diffuse gamma rays with  $140 \text{ TeV} < E < 1.3 \text{ PeV}$  [18].

In this Letter, we report on the detection of diffuse gamma rays with  $100 \text{ TeV} < E < 1 \text{ PeV}$  from the Galactic disk with the Tibet air shower array and muon detector array (Tibet AS+MD array) and present evidence for PeV cosmic rays being accelerated and confined in the Galaxy.

## II. EXPERIMENT

In order to observe high-energy gamma rays with high sensitivity, we started a new hybrid experiment using the surface AS array combined with the underground water-Cherenkov-type muon detector array at Yangbajing ( $90.522^\circ\text{E}$ ,  $30.102^\circ\text{N}$ ; 4300 m above sea level) in Tibet, China. The AS array, covering a large area of  $65700 \text{ m}^2$ , precisely measures the arrival direction and energy of each primary cosmic ray, while the underground muon detector array, with a detection area of  $3400 \text{ m}^2$  beneath the AS array, measures number of muons in each AS. Because an AS induced by a gamma-ray contains much less muons than an AS induced by a primary cosmic ray in the atmosphere, the muon detector array enables us to efficiently discriminate cosmic-ray background events from gamma-ray signals [19]. Based on this technique, we suppressed more than 99.9% of cosmic-ray background events above 100 TeV and succeeded in detecting unprecedentedly high-energy gamma rays from the Crab Nebula. For more details, please see [12].

## III. DATA ANALYSIS

The energy and arrival direction of each gamma ray are reconstructed using the AS particle density and timing recorded at each scintillation detector composing the AS array. The angular resolution (50% containment) is estimated to be approximately  $0.22^\circ$  and  $0.16^\circ$  for 100 and 400 TeV gamma rays, respectively. The pointing accuracy has been estimated to be less than  $0.06^\circ$  from the observation of the Crab Nebula as described in the Supplemental Material of our previous Letter [12].

To estimate the gamma-ray energy, we use S50 defined as the particle density detected in an AS surface detector ( $\rho$ ) at a perpendicular distance of 50 m from the AS axis in the best-fit NKG function [20]. The energy resolutions with S50 are roughly estimated to be 20% and 10% for 100 TeV and 400 TeV, respectively. The absolute energy scale uncertainty was estimated to be 12% from the westward displacement of the Moon’s shadow center due to the geomagnetic field [21]. The live time of the dataset

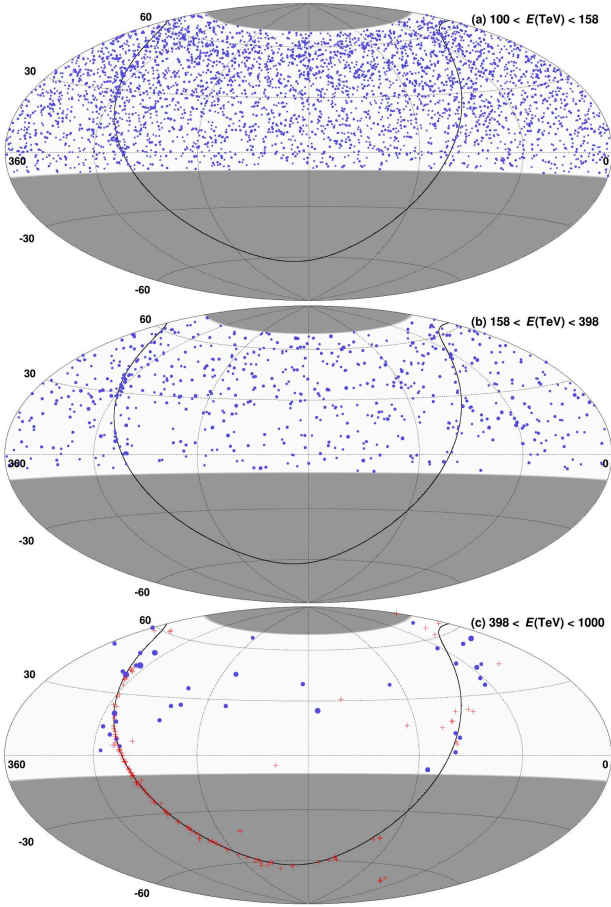


FIG. 1. The arrival direction of each gamma-ray-like event observed with (a)  $100 < E < 158$  TeV, (b)  $158 < E < 398$  TeV, and (c)  $398 < E < 1000$  TeV, respectively, in the equatorial coordinate. The blue solid circles show arrival directions of gamma-ray-like events observed by the Tibet AS+MD array. The area of each circle is proportional to the measured energy of each event. The red plus marks show directions of the known Galactic TeV sources (including the unidentified sources) listed in the TeV gamma-ray catalog [9]. The solid curve indicates the Galactic plane, while the shaded areas indicate the sky regions outside the field of view of the Tibet AS+MD array.

is 719 days from February 2014 to May 2017, and the average effective detection time for the Galactic plane observation is approximately 3700 hours at the zenith angle less than  $40^\circ$ . The data selection criteria are the same in our previous work [12] except for the muon cut condition. According to the CASA-MIA experiment, the marginal excess along the Galactic plane in the sub-PeV energies is  $1.63\sigma$  and the fraction of excess to cosmic-ray background events is estimated to be approximately  $3 \times 10^{-5}$  [18]. In order to search for signals with such a small excess fraction, we adopt a tight muon cut in the present analyses requiring for gamma-ray-like events to satisfy  $\Sigma N_\mu < 2.1 \times 10^{-4}$  ( $\Sigma \rho$ )<sup>1,2</sup> or  $\Sigma N_\mu < 0.4$ , where  $\Sigma N_\mu$  is the total number of muons detected in the un-

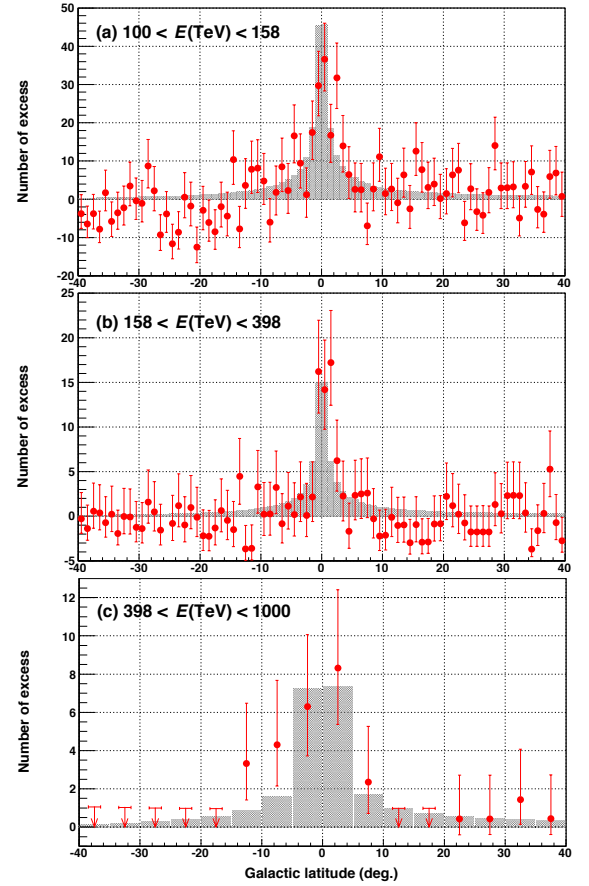


FIG. 2. Gamma-ray excess counts as a function of Galactic latitude with (a)  $100 < E < 158$  TeV, (b)  $158 < E < 398$  TeV, and (c)  $398 < E < 1000$  TeV, respectively. The excess count is calculated from the observed event number after subtracting the estimated background event number (see text). The Galactic longitude of the arrival direction in each figure is integrated across our FOV (approximately  $22^\circ < l < 225^\circ$ ). The solid circles show the experimental data, while the shaded histograms display the model profile [8] rebinned in every (a)(b)  $1^\circ$  and (c)  $5^\circ$  of the Galactic latitude. The downward arrows show upper limits of excess at 68% confidence level. The number of excess in the model, which is independent of energy, is normalized to the observed number within  $|b| < 5^\circ$ .

derground muon detector array. This is just one order of magnitude tighter than the criterion used in our previous work [12]. The cosmic-ray survival ratio with this tight muon cut is experimentally estimated to be approximately  $10^{-6}$  above 400 TeV, while the gamma-ray survival ratio is estimated to be 30% by the MC simulation. The comparison between the cosmic-ray data and the MC simulation is described in Fig. S1 in Supplemental Material [37].

#### IV. RESULTS AND DISCUSSION

Figure 1 shows arrival directions of gamma-ray-like events in (a)  $100 (= 10^{2.0}) < E < 158 (= 10^{2.2})$  TeV, (b)  $158 (= 10^{2.2}) < E < 398 (= 10^{2.6})$  TeV and (c)  $398 (= 10^{2.6}) < E < 1000 (= 10^{3.0})$  TeV, remaining after the tight muon cut. It is seen that the observed arrival directions concentrate in a region along the Galactic plane (see also Fig. 2). Particularly in Fig. 1 (c), 23 gamma-ray-like events are observed in  $|b| < 10^\circ$  which we define as the ON region ( $N_{\text{ON}} = 23$ ), while only 10 events are observed in  $|b| > 20^\circ$  which we define as the OFF region ( $N_{\text{OFF}} = 10$ ). Since the total number of events before the tight muon cut is  $8.6 \times 10^6$ , the cosmic-ray survival ratio is estimated to be  $1.2 \times 10^{-6}$  in  $|b| > 20^\circ$  above 398 TeV. We use  $N_{\text{OFF}}$  in  $|b| > 20^\circ$  to estimate the number of cosmic-ray background events, because the contribution from extragalactic gamma rays in  $E > 100$  TeV is expected to be strongly suppressed due to the pair-production interaction with the extragalactic background light. The mean free path lengths for the pair-production for 100 TeV and 1 PeV are a few Mpc and 10 kpc, respectively [22].

Since the ratio ( $\alpha$ ) of exposures in ON and OFF regions is estimated to be 0.27 by the MC simulation with our geometrical exposure, the expected number of background events in the ON region with  $|b| < 10^\circ$  is  $N_{\text{BG}} = \alpha N_{\text{OFF}} = 2.73$  and the Li-Ma significance [23] of the diffuse gamma rays in the ON region is calculated to be  $5.9\sigma$ . The number of events and the significances in each energy bin are summarized in Table S1 in Supplemental Material [37]. The observed distribution of the number of muons for  $E > 398$  TeV after the muon cut is consistent with that estimated from the gamma-ray MC simulation as shown in Fig. S2 in Supplemental Material [37]. The highest energy  $957^{+166}_{-141}$  TeV gamma ray is observed near the Galactic plane, where the uncertainty in energy is defined as the quadratic sum of the absolute energy-scale error (12%) and the energy resolution [12]. Solid circles in Fig. 2 display  $N_{\text{ON}} - N_{\text{OFF}}$  as a function of  $b$  in (a)  $100 < E < 158$  TeV, (b)  $158 < E < 398$  TeV, and (c)  $398 < E < 1000$  TeV. The concentration of diffuse gamma rays around the Galactic plane is apparent particularly in Fig. 2.

In order to estimate contribution from the known gamma-ray sources, we searched for gamma-ray signals above 100 TeV from the direction of the selected 60 Galactic sources (excluding the extragalactic-type sources, but including the unidentified (UNID) sources) listed in the TeV source catalog [9] within  $|b| < 5^\circ$  in our field of view (FOV). We used a search window with a radius of  $0.5^\circ$  centered at each source direction, which contains more than 90% of gamma-ray events, as shown in Fig. S3 in Supplemental Material [37]. Since the source extensions of the HAWC sources above 56 TeV were typically around  $0.3^\circ$  [13], the search window radius  $0.5^\circ$  is appropriate to exclude most of the contributions from such extended sources to diffuse gamma rays. Stacking 60 sources, we found 37 gamma-ray-like events within

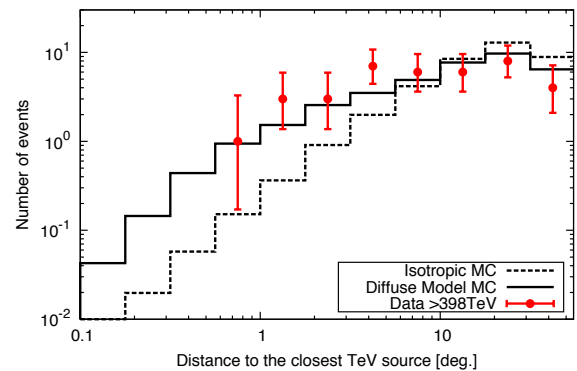


FIG. 3. The distribution of the angular distance between the arrival direction of each observed gamma-ray-like event with  $E > 398$  TeV and the direction of its closest known TeV source listed in the TeV gamma-ray catalog [9]. The red solid circles show the observed data, while the dashed and solid histograms display the MC results expected from the isotropic event distribution and the diffuse gamma-ray model [8], respectively, to be observed with our geometrical exposure.

search windows against 8.7 background events, which corresponds to  $6.8\sigma$  above 100 TeV, while the number of all excess within  $|b| < 5^\circ$  ( $N_{\text{excess}}$ ) is 253.5. The fractional source contribution ( $N_{\text{point}} = 37 - 8.7 = 28.3$ ) to the diffuse component ( $N_{\text{diffuse}} = N_{\text{excess}} - N_{\text{point}} = 225.2$ ) is estimated to be 13% above 100 TeV.

We also searched for gamma-ray signals within a search window centered at each direction of 38 gamma-ray-like events in  $E > 398$  TeV, but we found no significant signal above 10 TeV. This implies that these 38 events are orphan gamma rays as is expected from the diffuse gamma-ray scenario, although the existence of unknown sporadic/weak steady sources with very hard spectra in each direction cannot be ruled out.

Figure 3 shows the distribution of angular distance between each of 38 gamma-ray-like events in  $E > 398$  TeV and its closest Galactic TeV source. Surprisingly, there is no gamma-ray excess near the know TeV sources. Such high-energy gamma rays which originate from PeV electrons should be produced near by the sources, due to significant energy loss via the synchrotron radiation in the magnetic field around the source. The observed gamma rays are, therefore, hard to interpret in the leptonic scenario. The gamma-ray emission by electrons will be also significantly suppressed above 100 TeV due to rapid decrease of Inverse-Compton (IC) cross section by the Klein-Nishina effect.

Recently, Lipari and Vernetto [8] developed a model capable of successfully reproducing the diffuse gamma-ray/neutrino flux observed in  $0.1 \text{ GeV} < E < 10 \text{ PeV}$ , by utilizing relevant cosmic-ray nuclei and electron spectra, interstellar gas distribution, soft photon field, gamma-ray/neutrino production processes and absorption effects in the Galaxy. They tested two different models named the space-independent and space-dependent models. The



cosmic-ray spectrum in the first model is assumed to be identical everywhere in the Galaxy, while the spectrum in the second model is assumed to be harder in the central region of the Galaxy than that at the Earth as indicated by the observed spectral index of Galactic diffuse gamma rays in  $0.1 < E < 100$  GeV. This kind of scenario was also discussed elsewhere [24]. Both models can reproduce the observed flux and spatial distribution of arrival directions by *Fermi*-LAT in the GeV energy region. The predicted gamma-ray spectrum above 1 GeV is also dominated by the contribution from the hadronic interaction between the interstellar matter and cosmic rays. It was concluded that the contribution to the diffuse gamma rays from the IC scattering and bremsstrahlung by relativistic electrons is less than 5% compared with the hadronic process above 100 TeV, considering the steep electron and positron spectra with  $p = -3.8$  measured by HESS [25], DAMPE [26] and CALET [27]. Another model [28] showed the IC scattering contribution in the low Galactic latitude is negligible above 20 TeV.

Gray histograms in Fig. 2 show the prediction of the space-independent model [8]. It is seen that the distribution in (a)(b) is overall consistent with the model prediction. The distribution in (c) observed in  $398 < E < 1000$  TeV looks broader than that in (a)(b), but it is also statistically consistent with the prediction rebinned in every  $5^\circ$  of the Galactic latitude (b).

Figure 4 shows the observed differential energy spectra of diffuse gamma rays, compared with the model predictions by Lipari and Vernetto [8] in which gamma-ray spectra are calculated in (a)  $25^\circ < l < 100^\circ$  and (b)  $50^\circ < l < 200^\circ$  along the Galactic plane, each in  $|b| < 5^\circ$ . The measured fluxes by the Tibet AS+MD array are summarized in Table S2 in Supplemental Material [37]. These fluxes are obtained after subtracting events within  $0.5^\circ$  from the known TeV sources and the systematic error of the observed flux is approximately 30% due to the uncertainty of absolute energy-scale [21]. We corrected time variation of detector gain at each detector based on the single particle measurement for each run. The time variation of gamma-ray-like excess above 100 TeV in  $|b| < 5^\circ$  is stable within approximately 10%. It is seen that the measured fluxes by the Tibet AS+MD array are compatible with both the space-independent and space-dependent models based on the hadronic scenario. As a leptonic model, it is proposed that gamma-ray halos induced by the relativistic electrons and positrons from pulsars explain the Galactic diffuse gamma rays above 500 GeV [29]. However, the gamma-ray flux predicted by this model has an exponential cutoff well below 100 TeV, and is inconsistent with the observation by Tibet AS+MD array (see Fig. 4(a)).

The observed flux in the highest energy bin in  $398 < E < 1000$  TeV looks higher than the model prediction, but it is not inconsistent with the model when the statistical and systematic errors are considered. Above 398 TeV, the total number of observed events is 10 in each of  $25^\circ < l < 100^\circ$  and  $50^\circ < l < 200^\circ$ , which includes

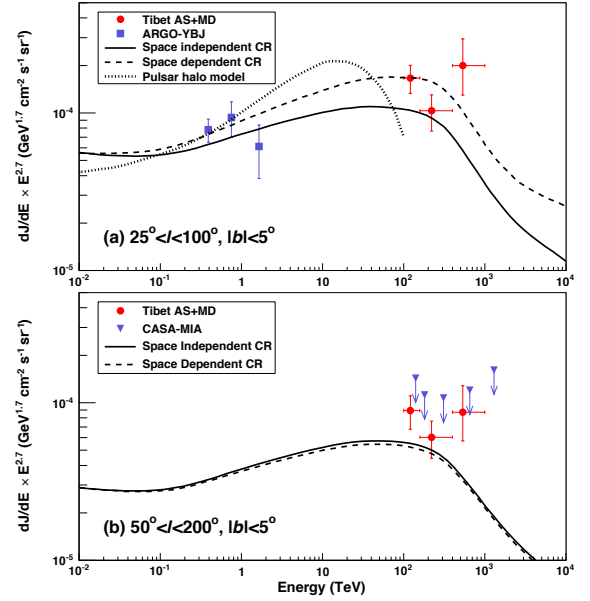


FIG. 4. Differential energy spectra of the diffuse gamma rays from the Galactic plane in the regions of (a)  $|b| < 5^\circ$ ,  $25^\circ < l < 100^\circ$  and (b)  $|b| < 5^\circ$ ,  $50^\circ < l < 200^\circ$ , respectively. The solid circles show the observed flux after excluding the contribution from the known TeV sources listed in the TeV gamma-ray catalog [9], while the solid and dashed curves display the predicted energy spectra by the space-independent and space-dependent models by Lipari and Vernetto [8], respectively (see text). The dotted curve in panel (a) shows the flux predicted by a leptonic model [29] in which gamma rays are induced by relativistic electrons and positrons from pulsars. Solid squares in panel (a) and triangles with arrows in panel (b) indicate the flux measured by ARGO-YBJ [17] and the flux upper limit by the CASA-MIA experiment [18], respectively. The error bar shows  $1\sigma$  statistical error.

the Cygnus region around  $l = 80^\circ$ . Interestingly, 4 out of 10 events are detected within  $4^\circ$  from the center of the Cygnus cocoon, which is claimed as an extended gamma-ray source by the ARGO-YBJ [30] and also proposed as a strong candidate of the PeVatrons [31], but not taken into account in the model [8]. If these 4 events are simply excluded, the observed flux at the highest energy in Fig. 4 better agrees with model predictions.

The high-energy astrophysical neutrinos are also a good probe of the spectrum and spatial distribution of PeV cosmic rays in the Galaxy [32, 33]. According to Lipari and Vernetto [8], the diffuse gamma-ray/neutrino fluxes predicted near the Galactic center ( $|l| < 30^\circ$ ) by the space-dependent model are more than 5 times higher than that predicted by the space-independent model in  $100 \text{ TeV} < E < 10 \text{ PeV}$ . Therefore, the gamma-ray/neutrino observations in the southern hemisphere will also play important roles to understand or constrain the spatial distribution of PeV cosmic rays in the Galaxy. Probing PeV diffuse gamma rays/neutrinos from the large-scale structures, such as the Fermi-bubble [34] and

the possible dark matter halo in the Galaxy [35, 36], will be also interesting.

## V. CONCLUSIONS

We successfully observed the Galactic diffuse gamma rays in  $100 \text{ TeV} < E < 1 \text{ PeV}$  by the Tibet AS+MD array. Particularly, in the energy region above 398 TeV, we found 23 gamma-ray-like events against 2.73 background events, which corresponds to  $5.9\sigma$  statistical significance, in  $|b| < 10^\circ$  in our FOV. The highest energy of the observed gamma ray is  $957^{(+166)}_{(-141)} \text{ TeV}$ , which is nearly 1 PeV. The gamma-ray distribution are extended around the Galactic plane apart from known Galactic TeV gamma-ray sources. We also found no significant signal above 10 TeV in directions of 38 gamma-ray-like events above 398 TeV, which implies that these events are orphan gamma rays as is expected from the diffuse gamma-ray scenario. The measured fluxes are overall consistent with recent models assuming the hadronic cosmic-ray origin. These facts are hard to interpret with the leptonic cosmic-ray origin, indicating that sub-PeV diffuse gamma rays are produced by the hadronic interaction of protons, which are accelerated up to a few PeV energies (or possibly  $\sim 10 \text{ PeV}$ ) and escaping from the source, with the interstellar gas in our Galaxy. Hence, we conclude that the PeVatrons inevitably exist in the present and/or past Galaxy accelerating cosmic rays which spread in the Galaxy being well confined around the Galactic disk.

## ACKNOWLEDGMENTS

The collaborative experiment of the Tibet Air Shower Arrays has been conducted under the auspices of the Ministry of Science and Technology of China and the Ministry of Foreign Affairs of Japan. This work was supported in part by a Grant-in-Aid for Scientific Research on Priority Areas from the Ministry of Education, Culture, Sports, Science and Technology, and by Grants-in-Aid for Science Research from the Japan Society for the Promotion of Science in Japan. This work is supported by the National Key R&D Program of China (No. 2016YFE0125500), the Grants from the National Natural Science Foundation of China (Nos. 11533007, 11673041, and 11873065), and the Key Laboratory of Particle Astrophysics, Institute of High Energy Physics, CAS. This work is also supported by the joint research program of the Institute for Cosmic Ray Research (ICRR), the University of Tokyo.

<sup>†</sup> Deceased

Corresponding authors:

\* kawata@icrr.u-tokyo.ac.jp

‡ huangjing@ihep.ac.cn

¶ takita@icrr.u-tokyo.ac.jp

§ chending@bao.ac.cn

- 
- [1] J. R. Hörandel, *Astropart. Phys.* **19**, 193 (2003).
  - [2] G. V. Kulikov and G. B. Khristiansen, *J. Exp. Theor. Phys.* **35**, 635 (1958).
  - [3] M. Amenomori *et al.*, *Astrophys. J.* **678**, 1165 (2008).
  - [4] E. G. Berezhko and L. G. Ksenofontov, *J. Exp. Theor. Phys.* **89**, 391 (1999).
  - [5] K. Kobayakawa *et al.*, *Phys. Rev. D* **66**, 083004 (2002).
  - [6] S. R. Kelner, F. A. Aharonian, and V. V. Bugayov, *Phys. Rev. D* **74**, 034018 (2006).
  - [7] A. Kappes, J. Hinton, C. Stegmann, and F. A. Aharonian, *Astrophys. J.* **656**, 870 (2007).
  - [8] P. Lipari and S. Vernetto, *Phys. Rev. D* **98**, 043003 (2018).
  - [9] S. Wakely and D. Horan,  
available at <http://tevcat.uchicago.edu>.
  - [10] H. Abdalla *et al.*, *Astron. Astrophys.* **612**, A1 (2018).
  - [11] A. U. Abeysekara *et al.*, *Astrophys. J.* **843**, 40 (2017).
  - [12] M. Amenomori *et al.*, *Phys. Rev. Lett.* **123**, 051101 (2019).
  - [13] A. U. Abeysekara *et al.*, *Phys. Rev. Lett.* **124**, 021102 (2020).
  - [14] S. D. Hunter *et al.*, *Astrophys. J.* **481**, 205 (1997).
  - [15] M. Ackermann *et al.*, *Astrophys. J.* **750**, 3 (2012).
  - [16] R. Atkins *et al.*, *Phys. Rev. Lett.* **95**, 251103 (2005).
  - [17] B. Bartoli *et al.*, *Astrophys. J.* **806**, 20 (2015).
  - [18] A. Borione *et al.*, *Astrophys. J.* **493**, 175 (1998).
  - [19] T. K. Sako a, K. Kawata, M. Ohnishi, A. Shiomi, M. Takita and H. Tsuchiya, *Astropart. Phys.* **32**, 177 (2009).
  - [20] K. Kawata, T. K. Sako, M. Ohnishi, M. Takita, Nakamura and K. Munakata, *Exp. Astron.* **44**, 1 (2017).
  - [21] M. Amenomori *et al.*, *Astrophys. J.* **692**, 61 (2009).
  - [22] R. J. Protheroe and H. Meyer, *Phys. Lett. B* **493**, 1 (2000).
  - [23] T.-P. Li and Y.-Q. Ma, *Astrophys. J.* **272**, 317 (1983).
  - [24] Y. Q. Guo and Q. Yuan, *Phys. Rev. D* **97**, 063008 (2018).
  - [25] F. A. Aharonian *et al.*, *Phys. Rev. Lett.* **101**, 261104 (2008).
  - [26] G. Ambrosi *et al.*, *Nature* **552**, 63 (2017).
  - [27] O. Adriani *et al.*, *Phys. Rev. Lett.* **120**, 261102 (2018).
  - [28] D. Gaggero, D. Grasso, A. Marinelli, A. Urbano, and M. Valli, *Astrophys. J.* **815**, L25 (2015).
  - [29] T. Linden and B. J. Buckman, *Phys. Rev. Lett.* **120**, 121101 (2018).
  - [30] B. Bartoli *et al.*, *Astrophys. J.* **790**, 152 (2014).
  - [31] F. Aharonian, R. Yang and E. de Oña Wilhelmi, *Nat. Astron.* **3**, 561 (2019).
  - [32] A. Albert *et al.*, *Astrophys. J.* **868**, L20 (2018).
  - [33] M. G. Aartsen *et al.*, *Astrophys. J.* **886**, 12 (2019).
  - [34] L. Yang and S. Razzaque, *Phys. Rev. D* **99**, 083007 (2019).

- [35] A. Esmaili and P. D. Serpico , J. Cosmol. Astropart. Phys. **11**, 054 (2013).
- [36] K. Murase, R. Laha, S. Ando, and M. Ahlers, Phys. Rev. Lett. **115**, 071301 (2015).
- [37] See Supplemental Material for supporting figures and tables, which includes Refs. [12,19,38-43].
- [38] D. Heck, J. Knapp, J. N. Capdevielle, G. Shatz and T. Thouw, CORSIKA: A Monte Carlo Code to Simulate Extensive Air Showers (FZKA 6019)(Karlsruhe: Forschungszentrum Karlsruhe) (1998).
- [39] T. Pierog, Iu Karpenko, J. M. Katzy, E. Yatsenko and K. Werner, Physical Review C **92**, 034906 (2015).
- [40] A. Ferrari, P. R. Sala, A. Fassò and J. Ranft, FLUKA: A multi-particle transport code, CERN-2005-10, INFN/TC\_05/11, SLAC-R-773 (2005).
- [41] T. T. Böhlen *et al.*, Nucl. Data Sheets **120**, 211 (2014).
- [42] S. Agostinelli *et al.*, Nucl. Instrum. Methods Phys. Res., Sect. A **506**, 250 (2003).
- [43] M. Shibata, Y. Katayose, J. Huang, and D. Chen, Astrophys. J. **716**, 1076 (2010).

TABLE S3. (Table in the Supplemental Material) Event IDs and arrival directions in the equatorial coordinates (Right Ascension, Declination) of the gamma-ray like events with  $398 < E < 1000$  TeV observed by the Tibet AS+MD array during period between February 2014 and May 2017.

TASG Event ID	R.A. J2000 (degrees)	Dec. J2000 (degrees)
TASG-D01-001	18.74	55.31
TASG-D01-002	26.44	68.23
TASG-D01-003	35.21	54.46
TASG-D01-004	49.16	44.38
TASG-D01-005	55.90	43.25
TASG-D01-006	62.31	38.11
TASG-D01-007	63.13	55.26
TASG-D01-008	63.72	34.74
TASG-D01-009	67.01	46.54
TASG-D01-010	96.16	9.02
TASG-D01-011	98.31	11.21
TASG-D01-012	99.60	1.58
TASG-D01-013	114.74	-7.55
TASG-D01-014	127.01	38.26
TASG-D01-015	174.45	24.48
TASG-D01-016	183.43	39.60
TASG-D01-017	228.12	26.53
TASG-D01-018	230.56	44.40
TASG-D01-019	243.22	66.27
TASG-D01-020	255.47	26.46
TASG-D01-021	256.49	35.31
TASG-D01-022	261.10	25.56
TASG-D01-023	264.29	17.95
TASG-D01-024	284.38	4.50
TASG-D01-025	286.96	7.96
TASG-D01-026	290.28	16.36
TASG-D01-027	291.45	10.03
TASG-D01-028	293.62	20.36
TASG-D01-029	295.63	2.30
TASG-D01-030	297.17	13.82
TASG-D01-031	305.44	44.21
TASG-D01-032	307.08	39.02
TASG-D01-033	308.69	43.92
TASG-D01-034	309.49	51.05
TASG-D01-035	312.33	40.23
TASG-D01-036	320.32	49.46
TASG-D01-037	354.97	49.65
TASG-D01-038	359.96	59.19